Eliashberg analysis of the optical conductivity in superconducting Pr_2CuO_x ($x \simeq 4$)

E Schachinger[1], G Chanda[2,3], R P S M Lobo[4,5,6], M Naito[7] and A V Pronin[2,8]

[1] Institute of Theoretical and Computational Physics, NAWI Graz, Graz University of Technology, A-8010 Graz, Austria
[2] Dresden High Magnetic Field Laboratory (HLD), Helmholtz-Zentrum Dresden-Rossendorf, 01314 Dresden, Germany
[3] Institut für Festkörperphysik, Technische Universität Dresden, 01062 Dresden, Germany
[4] LPEM, PSL Research University, ESPCI ParisTech, 10 rue Vauquelin, 75231 Paris Cedex 5, France
[5] CNRS, UMR8213, Paris, France
[6] Sorbonne Universités, UPMC Univ. Paris 6, 75005, Paris, France
[7] Department of Applied Physics, Tokyo University of Agriculture and Technology, Naka-cho 2-24-16, Koganei, Tokyo 184-8588, Japan
[8] A. M. Prokhorov Institute of General Physics, Russia Academy of Sciences, 119991 Moscow, Russia

E-mail: ewald.schachinger@live.at, pronin@ran.gpi.ru

Abstract. Superconducting Pr_2CuO_x, $x \simeq 4$ films with T' structure and a T_c of 27 K have been investigated by millimeter-wave transmission and broadband (infrared-to-ultraviolet) reflectivity measurements in the normal and superconducting state. The results obtained by both experimental methods show a consistent picture of the superconducting condensate formation below T_c. An Eliashberg analysis of the data proves d-wave superconductivity and unitary-limit impurity scattering of the charge carriers below T_c. The derived electron-exchange boson interaction spectral function $I^2\chi(\omega)$ shows only marginal changes at the superconducting transition with the mass enhancement factor λ, the first inverse moment of $I^2\chi(\omega)$, being equal to 4.16 at 30 K and to 4.25 at 4 K.

PACS numbers: 74.25.Gz, 74.25.nd, 74.72.Ek

1. Introduction

The parent compounds of the superconducting high-T_c cuprates are generally considered to be antiferromagnetic charge-transfer insulators (CTIs) [1, 2]. For the hole-doped compounds, this statement is commonly accepted. For the electron-doped cuprates, the situation is trickier: there are studies, that put a question mark on this picture.

For example, in 1995 Brinkmann *et al.* [3] demonstrated that the superconducting phase in $Pr_{2-x}Ce_xCuO_4$ (PCCO) single crystals can exist at doping levels as low as 4 %. This was achieved by a special oxygen-reduction and annealing technique. A large body of work performed in the last few years on thin films demonstrated that even the parent compounds of the electron-doped cuprates, e.g. $(La,Y)_2CuO_4$ and R_2CuO_4

with R being Pr, Sm, Nd, Eu, or Gd, are metallic and become superconducting at low temperatures [4, 5, 6, 7, 8, 9, 10, 11]. Finally, superconductivity was reported in nominally undoped polycrystalline samples of $(La,Sm)_2CuO_4$ [12, 13] and in heavily underdoped single crystals of the Pr-La-Ce-Cu-O system [14].

The sharp contradiction between these and earlier results can be explained as being due to structure-related issues, namely due to the presence or absence of oxygen atoms in apical positions, i.e. in positions directly above and below the copper atoms in the CuO_2 planes, as illustrated in the right-hand corner of Figure 1. While the hole-doped cuprates have the so-called T structure characterized by the presence of apical oxygen, the electron-doped cuprates are supposed to posses the T' structure, with no apical oxygen. In practice, though, it is very hard to remove the apical oxygen from the electron-doped cuprates completely, particularly in bulk samples [10]. Apical oxygen in the T' structure is known to act as a very strong scatterer and pair breaker [15] and, thus, the T_c reduction in the underdoped compounds may in fact be due to the remaining apical oxygen. Because of tenuity of films and their large surface-to-volume ratio, the process of removing extra oxygen (oxygen reduction) is easier to perform and control in films rather than in bulk samples. This makes films advantageous for achieving the proper T' structure with no apical oxygen.

Superconductivity reported in undoped cuprates challenges the applicability of the CTI picture to electron-doped cuprates [16]. It is worth noting here that recent calculations performed on the basis of a new first-principles method report a sharp difference between the parent compounds with T and T' structures [17, 18, 19]. While the first are found to be "standard" CTIs, the latter, e.g. Pr_2CuO_4, are essentially metallic and their apparent insulating nature may originate from magnetic long-range order (Slater transition) which is competing with the metallic ground state.

However, it is still an open question whether the supposedly undoped T' superconductors are truly undoped. An alternative possibility is a doping by oxygen vacancies in the RO layers. These vacancies may in principle be created during the oxygen-reduction process. Because no single-crystalline bulk T'-R_2CuO_4 superconducting samples have yet been synthesized, direct measurements of the oxygen distribution are impossible so far. Nevertheless, neutron diffraction experiments performed on $Nd_{2-x}Ce_xCuO_{4+y}$ single crystals showed that it was mostly apical oxygen, which was removed during the oxygen reduction [20, 21]. The recent report on superconductivity in bulk heavily underdoped T'-$Pr_{1.3-x}La_{0.7}Ce_xCuO_{4+\delta}$ gives hope that the oxygen distribution issue for the T' cuprates might be clarified in the near future [14].

In our recent paper [22] we investigated the optical response of MBE-grown Pr_2CuO_x (PCO) films with $x \simeq 4$. We showed that the optical response can be consistently understood within the picture in which superconductivity develops in undoped PCO, i.e. x is indeed 4. (Although it is quite obvious that one cannot judge whether or not the CTI picture is valid from optical measurements alone). In that paper, we reported on *normal-state* broadband optical reflectivity measurements and on millimeter-wave measurements below the superconducting transition. We demonstrated that neither raw experimental optical data nor their analysis reveal any indication of normal-state gap-like features which could be attributed to the existence of a normal-state pseudogap. This observation is in line with the breakdown of the CTI picture in PCO. In our millimeter-wave measurements, we directly observed the formation of the superconducting condensate at $T < T_c$ and found that the temperature dependence of the London penetration depth at low temperatures follows

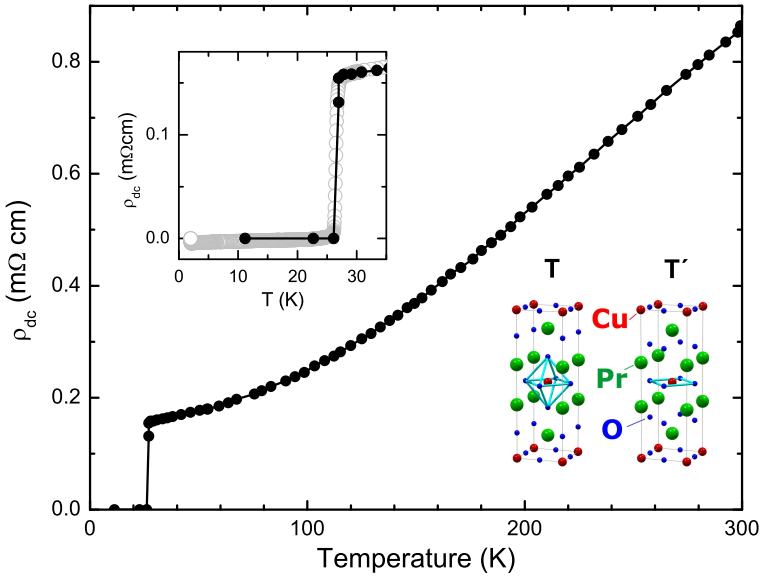

Figure 1. (Color online) Main panel: Temperature dependence of the in-plane dc resistivity ρ_{dc} of the T'-PCO film. In the right-hand corner schematic diagrams illustrate the T and T' structures. Inset: A close-up of the dc resistivity around the superconducting transition. The dc measurements were performed twice: on the fresh film [solid (black) symbols] and after completion of all optical measurements [open (grey) symbols].

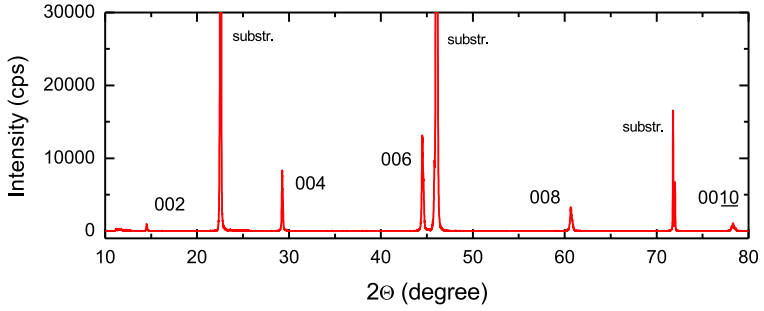

Figure 2. (Color online) X-ray diffraction pattern of a c-axes oriented PCO film on $DyScO_3$ substrate. Diffraction peaks coming from the substrate are marked as "substr." The lattice constant along the c-axes calculated from the positions of the film peaks is 12.20 Å, indicating the optimal oxygen reduction and the proper T' structure [4].

a quadratic power law indicating a d-wave pairing symmetry typical for cuprate superconductors. Similar results on penetration depth for PCO films, prepared by metalorganic decomposition, were also reported by some of us a few years earlier [23].

In this paper, we report on the broadband optical conductivity *in the superconducting state*, measured on the same sample as in Ref. [22]. We perform Eliashberg analysis of optical data collected below T_c and compare the results to the normal-state data of Ref. [22]. We demonstrate that the results obtained by both our techniques (broadband optical reflectivity and millimeter-wave transmission

measurements) for the superconducting state reveal a consistent picture of the superconducting condensate formation. We find that d-wave superconductivity and unitary-limit electron scattering off impurities describe best the available experimental data below T_c.

2. Samples and Experiment

As described in Ref. [22], the PCO films were grown by molecular beam epitaxy (MBE) [8] on a (110)-oriented 0.35 mm thick $DyScO_3$ substrate. The films were 100 nm thick with the c-axis oriented perpendicular to the film's surface. We investigated two thin films of PCO. The results, obtained on the films, do not demonstrate any significant difference. Hereafter we discuss results gathered from one of the two films, the same one as in Ref. [22].

Figures 1 and 2 show the results of dc resistivity and x-ray diffraction measurements performed on the film. The sharp diffraction peaks with no signs of spurious phases demonstrate the film's quality. The resistivity decreases monotonically with decreasing temperature down to $T_c = 27$ K. The width of the superconducting transition is 0.8 K. The T_c and the transition width remained unchanged after completion of all optical measurements (as evident from the inset of Figure 1) indicating that the film did not degrade in the course of our measurements.

We measured near-normal reflectivity from 40 to 55000 cm^{-1} at selected temperatures from 4 to 300 K and phase-sensitive transmission at 210 and 250 GHz (7 and 8.3 cm^{-1}) as a function of temperature, using backward wave oscillators (BWOs). Details of these measurements have been discussed by us earlier [22].

3. Experimental results

Figure 3 shows the in-plane (ab-plane) reflectivity of the PCO film on a $DyScO_3$ substrate versus frequency at 4 K and 30 K, e.g. at the lowest possible T in the superconducting state and at a temperature slightly above the T_c. At low frequencies, the reflectivity is quite high, typical for metals and metallic films. At 100 – 700 cm^{-1}, a number of phonon modes from both, the substrate and the film, affect the spectra. From 1000 to 10000 cm^{-1}, the reflectivity monotonously decreases with frequency. The maxima seen above 10000 cm^{-1} are due to inter-band transitions [22].

The inset of Figure 3 discusses the ratio R_s/R_n of the reflectivity at 4 K (R_s) and 30 K (R_n). Changes in the spectrum induced by the superconducting transition are not very pronounced but, nevertheless, can clearly be seen at frequencies below 200 cm^{-1}. If we reduce the frequency resolution [thick (black) line] the changes become more apparent. Let us emphasize, though, that because of the fact that the film is thin and partly transparent (the absolute reflectivity at low frequencies is only about 0.8) pronounced changes in the reflectivity induced by superconductivity cannot be expected in contrast to what can be observed in bulk samples.

For conventional isotropic s-wave superconductors the maximum in R_s/R_n is known to indicate the position of the superconducting energy gap $2\Delta_0$ [24]. For a rough estimate of $2\Delta_0$ such an approach can also be applied to the cuprates. If we associate in a straightforward way the maximum in R_s/R_n to the energy gap, then we obtain $2\Delta_0 = 110$ cm^{-1} and $2\Delta_0/k_BT_c = 5.8$. This value is roughly in the middle of the broad range of $2\Delta_0/k_BT_c$ obtained by different experimental methods for the

electron-doped cuprates [2] and is close to the results of optical measurements on PCCO with different doping levels [25, 26].

The film's complex optical conductivity, $\sigma = \sigma_1 + i\sigma_2$, has been extracted from the reflectivity spectra by use of a thin-film Drude-Lorentz fitting procedure which was described in necessary detail by Chanda *et al.* [22]. This procedure is similar to the one proposed by Kuzmenko [27] and can be as accurate as the Kramers-Kronig analysis (which is hardly possible for partly-transparent films on substrates). Neither BWO data nor values of the dc conductivity in the normal state have been utilized within this fitting procedure.

The real part of the PCO optical conductivity obtained by this modeling at 4 K and 30 K is presented in Figure 4. The lowest frequency of the reflectivity measurements was 40 cm^{-1}. Therefore, the data obtained from this analysis below this threshold frequency is to be considered as an extrapolation and is indicated by dashed lines as a guide to the eye. Nevertheless, the zero-frequency limit of σ_1 at 30 K evolves in accordance with σ_{dc} [(red) triangle on the vertical left-hand axis of Figure 4]. At low frequencies, the superconducting-state $\sigma_1(\omega)$ is below its normal state values. However, a large Drude-like contribution persists in the superconducting state. Similar behavior of optical conductivity has also been reported e.g. for $La_2Sr_{2-x}CuO_4$ [28] and $Bi_2Sr_2CaCu_2O_{8+\delta}$ [29, 30].

The inset of Figure 4 presents the data of the imaginary part of the optical conductivity, $\sigma_2(\omega)$, at 4 K [(black) line] and 30 K [(red) line]. In addition, the independent BWO data at 7 and 8.3 cm^{-1} are indicated by solid circles and it is

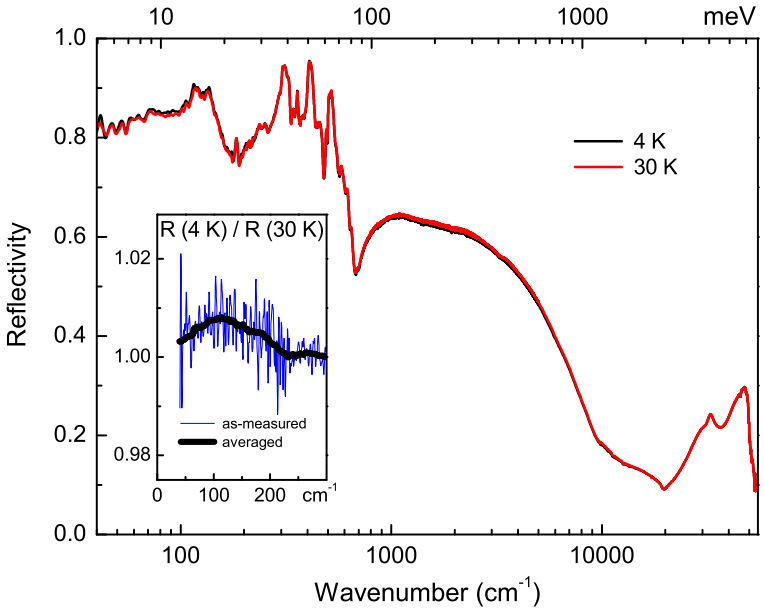

Figure 3. (Color online) Reflectivity of the PCO thin film on a $DyScO_3$ substrate as a function of frequency at 4 and 30 K. The **E** vector of the probing radiation lies in the *ab*-plane of the film (and parallel to the [001] axis of the substrate). The inset shows the superconducting-state (4 K) reflectivity divided by the normal-state (30 K) reflectivity at the lowest frequencies. The thin (blue) line corresponds to the measured and the thick (black) line to the frequency averaged spectrum.

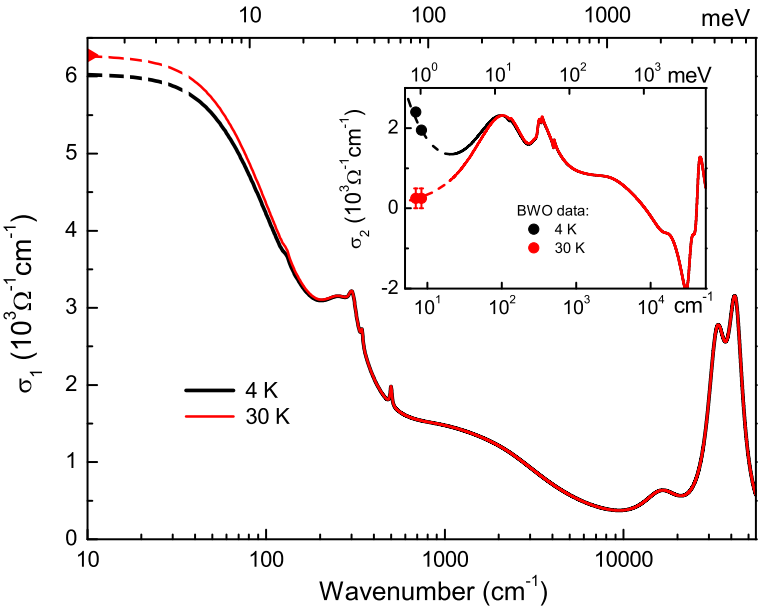

Figure 4. (Color online) Real (main panel) and imaginary (inset) part of the optical conductivity of PCO as a function of frequency for 4 [(black) lines] and 30 K [(red) lines]. The (red) right-hand triangle on the left-hand axis of the main panel represents the dc-conductivity at 30 K. Solid circles in the inset indicate $\sigma_2(\omega)$ data as obtained from the BWO phase-sensitive transmission measurements at 7 and 8.3 cm^{-1}. Error bars for the $T = 4$ K BWO data are within symbol size. The dashed lines starting below 40 cm^{-1} correspond to extrapolations obtained from the Drude-Lorentz fitting procedure as described by Chanda *et al.* [22].

evident that at $T = 4$ K $\sigma_2(\omega)$ tends to diverge for $\omega \to 0$, while at $T = 30$ K $\sigma_2(\omega)$ tends to zero within the same limit. Thus, our data for the superconducting and normal state are not only distinct from each other but they also exhibit the expected behavior [24] in the superconducting state: a divergence at $\omega \to 0$, and in the normal state: a Drude metal with diminishing $\sigma_2(\omega)$ at $\omega \to 0$.

4. Data Analysis

We start our analysis with the so-called extended Drude model [31, 32]. In this model the complex conductivity is given by

$$\sigma(\omega) = \frac{1}{4\pi} \frac{\omega_p^2}{\Gamma(\omega) - i\omega[1 + \lambda(\omega)]}, \tag{1}$$

where $[1 + \lambda(\omega)] = m^*(\omega)/m$ and $\tau_{op}^{-1}(\omega) \equiv \Gamma(\omega)$ are the frequency-dependent mass renormalization factor and the optical scattering rate, respectively. Inverting equation (1) gives:

$$1 + \lambda(\omega) = \frac{\omega_p^2}{4\pi} \frac{\sigma_2(\omega)}{\omega |\sigma(\omega)|^2}; \quad \Gamma(\omega) = \frac{\omega_p^2}{4\pi} \frac{\sigma_1(\omega)}{|\sigma(\omega)|^2}. \tag{2}$$

The frequency-dependent optical scattering rate, as obtained from our data using (2) with $\omega_p = 2.19$ eV [22], is displayed in Figures 5(a,b) as a function of frequency

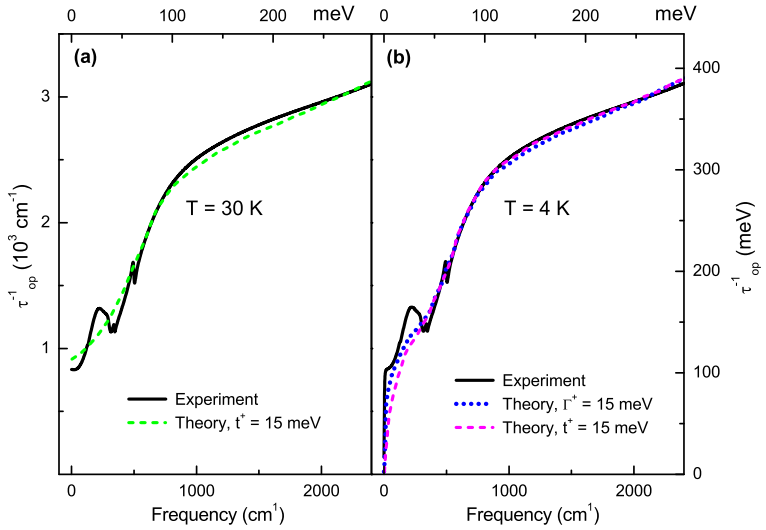

Figure 5. (Color online) The optical scattering rate $\tau_{op}^{-1}(\omega)$ vs energy ω. Frame (a): Normal state results at $T = 30\,\mathrm{K}$. The solid (black) curve represents the data while the dashed (green) line corresponds to the theoretical result of normal-state Eliashberg theory using the $I^2\chi(\omega)$ spectrum presented in Figure 6 by a dashed (black) line. The impurity parameter $t^+ = 15\,\mathrm{meV}$. Frame (b): Superconducting state results at $T = 4\,\mathrm{K}$. The solid (black) curve represents the data. The dotted (blue) line corresponds to results generated by d-wave symmetry Eliashberg theory on the basis of the $I^2\chi(\omega)$ spectrum presented in Figure 6 [solid (red) curve]. Impurity scattering was described in the unitary limit, $\Gamma^+ = 15\,\mathrm{meV}$. The dashed (magenta) curve presents the equivalent result for Born limit scattering with $t^+ = 15\,\mathrm{meV}$. Definitions of t^+ and Γ^+ are given in the text.

for 30 K and 4 K [solid (black) curves], respectively. The general trend in $\tau_{op}^{-1}(\omega)$ is to increase with frequency, but this increase is non-monotonic. This is due to phonons and a localization mode seen as a bump at around 230 cm^{-1} as discussed by Chanda *et al.* [22].

There is only little difference between the 4 K and 30 K $\tau_{op}^{-1}(\omega)$ data. This is quite similar to what has been reported for PCCO by Schachinger *et al.* [33]. Nevertheless, it is important to emphasize that according to (2) and the results for $\sigma_2(\omega)$ (see inset of Figure 4) the normal-state $\tau_{op}^{-1}(\omega)$ stays finite in the limit $\omega \to 0$. On the other hand, it drops precipitately to zero in the rather narrow energy range of $\omega \in [0, \sim 50]\,\mathrm{cm}^{-1}$ at $T = 4\,\mathrm{K}$. To emphasize this feature we added a small negative offset to the frequency-scale in Figures 5(a,b).

The difference between total optical scattering rate and impurity scattering rate, i.e. $\tau_{op}^{-1}(\omega) - \tau_{imp}^{-1}$, is according to P. B. Allen [34] closely related to the electron-exchange boson interaction spectral density $I^2\chi(\omega)$ which is at the core of the normal and superconducting state Eliashberg theory [35]. Thus, it is of quite some interest to gain knowledge on $I^2\chi(\omega)$ by inverting this difference using methods which have been discussed in detail by Schachinger *et al.* [36]. It was, furthermore, demonstrated by Schachinger *et al.* [37] that any non-zero contribution to $I^2\chi(\omega)$ at some energy ω will always result in an increase of the optical scattering rate. Consequently the bump observed in the experimental optical scattering rate of PCO (Figure 5) at around 230 cm^{-1} ($\sim 28\,\mathrm{meV}$) cannot be caused by electron-exchange boson interaction and is,

therefore, not part of the conducting-electron background.

The inversion of the normal state $T = 30\,\mathrm{K}$ data using a maximum entropy method of inversion [37] has already been discussed in quite some detail by Chanda *et al.* [22] and resulted in an $I^2\chi(\omega)$ spectrum featuring a double peak structure followed by a deep valley and a hump at higher energies. We reproduce these results for comparison in Figure 5(a) which shows the experimental data by a solid (black) line and the data reconstruction due to normal-state Eliashberg theory by a dashed (green) line. The resulting $I^2\chi(\omega)$ is presented by a dashed (black) line in Figure 6. The low-energy peak is at $\sim 11\,\mathrm{meV}$ and the high energy peak can be found at $\sim 50\,\mathrm{meV}$. This inversion process resulted also in an impurity scattering rate of $\tau_{imp}^{-1} = 2\pi t^+ = 100\,\mathrm{meV}$ ($t^+ = 15\,\mathrm{meV}$) which is quite substantial but in reasonable agreement with what has been reported for the system PCCO [33]. Similar double peak spectra have been reported for PCCO by Schachinger *et al.* [33] and for $La_{1.83}Sr_{0.17}CuO_4$ (a hole doped cuprate) by Hwang *et al.* [38] both with a less pronounced low-energy peak. It is most likely that the bump around $\sim 28\,\mathrm{meV}$ in the PCO $\tau_{op}^{-1}(\omega)$ data is responsible that the low-energy peak is too pronounced in the PCO $I^2\chi(\omega)$ spectrum.

More information on $I^2\chi(\omega)$ can be gained from an inversion of superconducting state data together with a comparison between data and theory. An inversion of the $T = 4\,\mathrm{K}$ superconducting state optical scattering rate data should be possible [36], but the formula quoted there is only valid in the clean-limit case and cannot be applied here. The only possibility that remains is to use the $I^2\chi(\omega)$ spectrum for $T = 30\,\mathrm{K}$ as a starting point and to calculate the optical scattering rate in the superconducting state at $T = 4\,\mathrm{K}$ using the full d-wave Eliashberg theory [35]. The use of d-wave Eliashberg

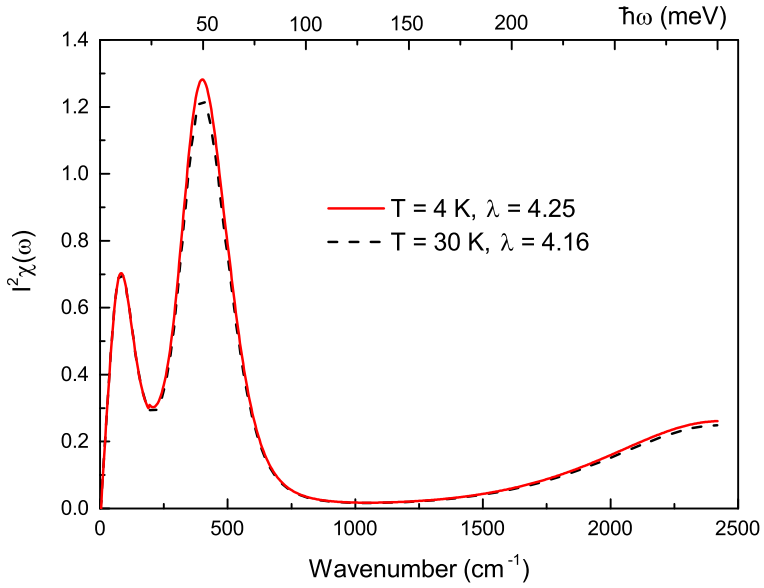

Figure 6. (Color online) The $I^2\chi(\omega)$ spectrum for two temperatures, namely $T = 4\,\mathrm{K}$ [solid (red) line] and $30\,\mathrm{K}$ [dashed (black) line] as a result of a straightforward inversion of the experimental $\tau_{op}^{-1}(\omega)$ data shown in Figure 5a. λ is the first inverse moment of $I^2\chi(\omega)$ or the mass enhancement factor.

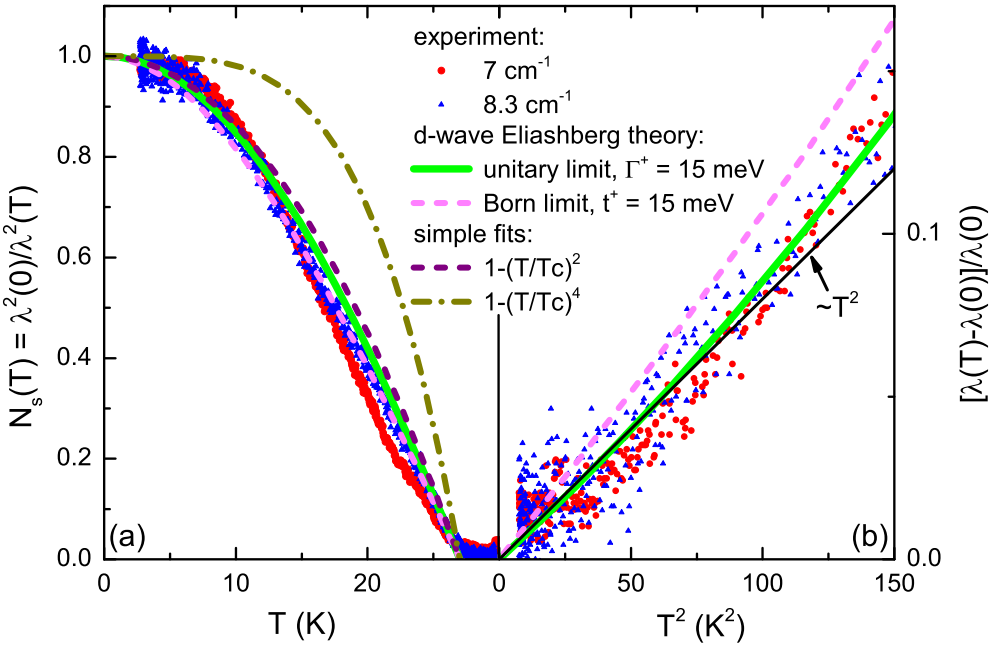

Figure 7. (Color online). Frame (a): Superfluid density, $N_s(T) = \lambda_L^2(0)/\lambda_L^2(T)$, as a function of temperature. Frame (b): Low-temperature variation of the normalized London penetration depth, $[\lambda_L(T) - \lambda_L(0)]/\lambda_L(0)$, as a function of temperature squared. Data derived from the millimeter-wave conductivity measurements at 7 cm^{-1} and 8.3 cm^{-1} are presented by solid (red) circles and solid (blue) triangles, respectively. Theoretical results generated by a full d-wave Eliashberg-theory calculation are shown for unitary scattering [thick solid (green) line] and Born limit scattering [think dashed (magenta) line]. Frame (a) contains for comparison the temperature dependence $N_s(T) = 1 - (T/T_c)^2$ [thin dashed (purple) line] which is expected for a nodal superconductor and $N_s = 1-(T/T_c)^4$ [thin dashed-dotted (olive) line] for a fully gaped superconductor. In Frame (b) a quadratic power law of the reduced penetration depth is indicated by a thin solid (black) line.

theory is justified by the fact that neither the superconducting-state data of $\sigma_1(\omega)$ nor the optical scattering rate show the signature of a full s-wave gap, where $\sigma_1(\omega)$ and $\tau_{op}^{-1}(\omega)$ would be equal to zero within the energy range $\omega \in [0, 2\Delta_0]$ with Δ_0 the superconducting gap. Moreover, the use of the normal state $I^2\chi(\omega)$ as a staring point is also justified by the fact that there is very little difference between the $T = 30\,\mathrm{K}$ and $4\,\mathrm{K}$ data except, of course, in the vicinity of $\omega = 0$. Thus, a least-squares fit procedure was employed to generate the superconducting state $I^2\chi(\omega)$ spectrum which allowed an optimum fit to the data. This spectrum is shown in Figure 6 by a solid (red) curve and is only marginally different from the corresponding normal-state derived spectrum. The mass enhancement factor λ also varies only little from 4.16 at $30\,\mathrm{K}$ to 4.25 at $4\,\mathrm{K}$.

Theory is compared with experiment in Figure 5(b). In contrast to the normal state, the scattering of the electrons off impurities is in the superconducting state more accurately described by a T-matrix approximation. Here, the impurity scattering rate is described by a parameter $\Gamma = 2\pi\Gamma^+ = n_I/[N(0)\pi^2]$ with n_I the concentration of scattering centers and $N(0)$ is the electronic density of states at the Fermi level. In

addition, there is a scattering phase shift δ_0 and we introduce an additional parameter $c = \cot(\delta_0)$ for convenience. The case $c = 0$ corresponds to unitary scattering and for $\delta_0 \to 0$, i.e. $c \to \infty$, the weak scattering limit (Born's approximation) is recovered [39]. (In the normal state only the weak scattering limit matters.) Consequently, Figure 5(b) presents results for unitary [dotted (blue) line] as well as Born limit scattering [dashed (magenta) line] off impurities. As in the normal state there is little agreement between theory and experiment in the energy range around the bump at $\sim 28\,\mathrm{meV}$. Nevertheless, it is obvious that theory with unitary scattering describes rather well the precipitous drop of $\tau_{op}^{-1}(\omega)$ to zero as $\omega \to 0$, while in the case of Born-limit scattering the decrease of $\tau_{op}^{-1}(\omega)$ as $\omega \to 0$ is more moderate.

If we want to discriminate even better between unitary and Born limit scattering we are required to analyze other experimental data which are linearly independent from the optical scattering rate data. One possibility is offered by the London penetration depth, $\lambda_L(T)$, derived from our phase-sensitive millimeter-wave transmission measurements [22]. From the theoretical point of view, $\lambda_L(T)$ can easily be calculated from d-wave Eliashberg theory using the $T = 4\,\mathrm{K}$ spectrum presented in Figure 6 together with the relevant impurity parameters because there is only little variation in the spectrum in going from 4 K to 30 K.

In Figure 7(a) we replot the temperature dependence of the normalized superfluid density, $N_s(T) = n_s(T)/n_s(0) = \lambda_L^2(0)/\lambda_L^2(T)$, which was obtained from millimeter-wave measurements at 7 cm^{-1} and 8.3 cm^{-1} and reported by us in Ref. [22]. Curves for $N_s(T) = 1-(T/T_c)^2$ and $N_s(T) = 1-(T/T_c)^4$ are added to mimic the temperature dependence of $N_s(T)$ for nodal (d-wave) and fully gaped (s-wave) superconductivity, respectively. As it has already been discussed in Ref. [22], the former curve describes the data reasonably well, whereas the fully-gaped behavior can be ruled out [40]. Here we added theoretical results gained from d-wave Eliashberg theory calculations for unitary scattering with $\Gamma^+ = 15\,\mathrm{meV}$ and Born limit scattering with $t^+ = 15\,\mathrm{meV}$. Both results agree reasonably well with experiment over the whole temperature range, thus supporting nodal superconductivity.

As we measure at a non-zero frequency, the normal electrons always contribute to λ_L. A comprehensive discussion on this issue is given in Ref. [41]. Obviously, the normal-electron contribution is minimal at the lowest T. Hence, the lowest-temperature behavior is most relevant for a comparison between experiment and theory which calculates λ_L in the $\omega \to 0$ limit. To provide this comparison, we plot the experimental and calculated low-temperature variation of the normalized penetration depth, $[\lambda_L(T)-\lambda_L(0)]/\lambda_L(0)$, as a function of the temperature squared in Figure 7(b). There is no question that the results for unitary scattering reproduce best the data. This result also agrees rather nicely with the findings reported by Schachinger *et al.* [33] for PCCO.

5. Conclusions

In our broadband investigation of the optical response of thin PCO films, we directly observed the formation of the superconducting condensate at $T < T_c$. Eliashberg analysis of the optical spectra and of the temperature dependence of the penetration depth proves PCO to be a rather dirty d-wave superconductor. In the superconducting state the scattering off impurities is best described within the unitary limit. The Eliashberg function $I^2\chi(\omega)$ develops only marginal changes in passing through T_c. Consequently, the mass enhancement factor λ changes very little from 4.16 at 30 K

and to 4.25 at 4 K. This is a rather big value but one has to keep in mind that scattering off impurities is pair-breaking in d-wave superconductors and a rather large value of λ is required to ensure a T_c of 27 K in our particular case.

Acknowledgments

We are very grateful to Dr. Hideki Yamamoto for his work on sample preparation and for useful discussions.

References

[1] Imada M, Fujimori A and Tokura Y 1998 *Rev. Mod. Phys.* **70** 1039
[2] Armitage N P, Fournier P and Greene R L 2010 *Rev. Mod. Phys.* **82** 2421
[3] Brinkmann M, Rex T, Bach H and Westerholt K 1995 *Phys. Rev. Lett.* **74** 4927
[4] Matsumoto O, Utsuki A, Tsukada A, Yamamoto H, Manabe T and Naito M 2009 *Phys. Rev.* B **79** 100508
[5] Matsumoto O, Utsuki A, Tsukada A, Yamamoto H, Manabe T and Naito M 2008 *Physica* C **468** 1148
[6] Matsumoto O, Tsukada A, Yamamoto H, Manabe T and Naito M 2010 *Physica* C **470** 1029
[7] Matsumoto O, Utsuki A, Tsukada A, Yamamoto H, Manabe T and Naito M 2009 *Physica* C **469** 924
[8] Yamamoto H, Matsumoto O, Krockenberger Y, Yamagami K and Naito M 2011 *Solid State Commun.* **151** 771
[9] Ikeda A, Matsumoto O, Yamamoto H, Manabe T and Naito M 2011 *Physica* C **471** 686
[10] Krockenberger Y, Irie H, Matsumoto O, Yamagami K, Mitsuhashi M, Tsukada A, Naito M and Yamamoto H 2013 *Sci. Rep.* **3** 2235
[11] Kojima K M, Krockenberger Y, Yamauchi I, Miyazaki M, Hiraishi M, Koda A, Kadono R, Kumai R, Yamamoto H, Ikeda A and Naito M 2014 *Phys. Rev.* B **89** 180508
[12] Ueda S, Asai S and Naito M 2010 *Physica* C **470** 1173
[13] Asai S, Ueda S and Naito M 2011 *Physica* C **471** 682
[14] Adachi T, Mori Y, Takahashi A, Kato M, Nishizaki T, Sasaki T, Kobayashi N and Koike Y 2013 *J. Phys. Soc. Jpn.* **82** 063713
[15] Sekitani T, Naito M and Miura N 2003 *Phys. Rev.* B **67** 174503
[16] Naito M, Matsumoto O, Utsuki A, Tsukada A, Yamamoto H and Manabe T 2008 *J. Phys.: Conf. Ser.* **108** 012037
[17] Das H and Saha-Dasgupta T 2009 *Phys. Rev.* B **79** 134522
[18] Weber C, Haule K and Kotliar G 2010 *Nat. Phys.* **6** 574
[19] Weber C, Haule K and Kotliar G 2010 *Phys. Rev. B* **82** 125107
[20] Schultz A J, Jorgensen J D, Peng J L, and Greene R L 1996 *Phys. Rev.* B **53** 5157
[21] Radaelli P G, Jorgensen J D, Schultz A J, Peng J L and R. L. Greene R L 1994 *Phys. Rev.* B **49** 15322
[22] Chanda G, Lobo R P S M, Schachinger E, Wosnitza J, Naito M and Pronin A V 2014 *Phys. Rev.* B **90** 024503
[23] Pronin A V, Fischer T, Wosnitza J, Ikeda A and Naito M 2012 *Physica* C **473** 11
[24] Tinkham M 1996 *Introduction to Superconductivity* (NY: Dover)
[25] Zimmers A, Lobo R P S M, Bontemps N, Homes C C, Barr M C, Dagan Y and Greene R L 2004 *Phys. Rev.* B **70** 132502
[26] Homes C C, Lobo R P S M, Fournier P, Zimmers A and Greene R L 2006 *Phys. Rev.* B **74** 214515
[27] Kuzmenko A B 2005 *Rev. Sci. Instrum.* **76** 083108
[28] Gorshunov B P, Pronin A V, Volkov A A , Somal H S, van der Marel D, Feenstra B J, Jaccard Y and Locquet J-P 2012 *Physica* B **244** 15
[29] Santander-Syro A F, Lobo R P S M, Bontemps N, Lopera W, Giratá D, Konstantinovic Z, Li Z Z and Raffy H 2004 *Phys. Rev.* B **70** 134504
[30] Corson J, Orenstein J, Oh S, ODonnell J, Eckstein J N 2000 *Phys. Rev. Lett.* **85** 2569
[31] Allen J W and Mikkelsen J C 1977 *Phys. Rev.* B **15** 2952
[32] Puchkov A V, Basov D N and Timusk T 1996 *J. Phys.: Condens. Matter* **8** 10049
[33] Schachinger E, Homes C C, Lobo R P S M and Carbotte J P 2008 *Phys. Rev.* B **78** 134522
[34] Allen P B 1971 *Phys. Rev.* B **3** 305

[35] Schachinger E and Carbotte J P 2003 Extended Eliashberg Theory for d-wave Superconductivity and Application to Cuprates *Models and Methods of High-T_c Superconductivity: Some Frontal Aspects* vol 2 (*Horizons in World Physics* vol 242) ed J K Srivastava and S M Rao (Hauppauge NY: Nova Science)
[36] Schachinger E, Neuber D and Carbotte J P 2006 *Phys. Rev.* B **73** 184507
[37] Schachinger E, Tu J J and Carbotte J P 2003 *Phys. Rev.* B **67** 214508
[38] Hwang J, Schachinger E, Carbotte J P, Gao F, Tanner D B and Timusk T 2008 *Phys. Rev. Lett.* **100** 137005
[39] Prohammer M, Perez-Gonzalez A and Carbotte J P, 1993 *Phys. Rev.* B **47** 15152
[40] Formally, a very small full gap cannot be excluded, because we do not measure at temperatures below 2.5 K.
[41] Dordevic S V, Singley E J, Basov D N, Komiya S, Ando Y, Bucher E, Homes C C and Strongin M 2002 *Phys. Rev.* B **65**, 134511